JOURNAL OF MATERIALS SCIENCE 24 (1989) 265–270

# $Ar^+$ ion beam induced silicide formation mechanism at the Pd–Si interface

C. N. WHANG, H. K. KIM
*Department of Physics, Yonsei University, Seoul 120, Korea*
R. Y. LEE
*Department of Materials Science and Engineering, Dankook University, Cheonahn 330, Korea*
R. J. SMITH
*Department of Physics, Montana State University, Bozeman, Montana 59717, USA*

Evaporated palladium films of 45 nm thickness on Si(1 1 1) were irradiated using 78 keV $Ar^+$ ions with doses in the range of $1 \times 10^{15}$ to $1.5 \times 10^{16}$ cm$^{-2}$ for the purpose of studying silicide formation. Rutherford backscattering analysis shows that intermixing has occurred across the Pd–Si interface at room temperature. The mixing behaviour increases with increasing dose of the bombarding ions, which agrees well with a theoretical model of isotropic cascade mixing for palladium, and radiation-enhanced diffusion associated with an interstitial mechanism for silicon.

## 1. Introduction

Irradiation of a solid with energetic particles can lead to the displacement of many target atoms away from their initial lattice sites. This process, often referred to as ion beam mixing (IBM), has been vigorously studied since about 1980. The enthusiasm for IBM has recently been stimulated by the expectation that IBM could find technological applications as a method for materials modification. For instance, the use of ion beams to induce metal–silicon reactions has received increasing attention in recent years. Compared to the conventional annealing method, the IBM process has several advantages [1] such as uniformity of the layer and reproducibility of the silicide growth associated with the interface cleaning action, and very low formation temperature due to the nucleated silicide.

The formation of metal-rich silicides such as $Pd_2Si$, $Pt_2Si$ and $Ni_2Si$ is particularly interesting from the viewpoints of both thermodynamics and practical applications since the reacted silicide films are known to be laterally uniform without any heat treatment after ion bombardment. Moreover, there are other interesting properties of the $Pd_2Si$ films formed on single-crystal Si(1 1 1); because of the near-matching of lattice constants, the films grow epitaxially on the Si(1 1 1) substrate by furnace annealing [2] or IBM [3], and the epitaxial $Pd_2Si$ films do not become amorphous on ion bombardment [4]. Furthermore, the formation of a PdSi phase by IBM at room temperature has received considerable attention for applications involving ohmic contacts and Schottky barriers in integrated circuit (IC) technology because a high formation temperature [5] ($> 700°$ C) is required in the normal annealing technique.

Previous related work includes that of Lee *et al.* [6] who reported some intermixing of palladium films on silicon after bombarding with phosphorus ions, and the observations by van der Weg *et al.* [7] of Pd/Si mixing using $Ar^+$ ions. Tsaur *et al.* [8] found that the $Pd_2Si$ phase was formed near the Pd–Si interface at low-dose $Xe^+$ ion bombardment, and a PdSi phase was formed near the $Pd_2Si$–Si interface at high doses of $Xe^+$ ion bombardment, or during subsequent thermal annealing at 300 to 400° C. Also, Ishiwara [3] observed the epitaxial growth of $Pd_2Si$ films on a Si(1 1 1) substrate using $Ar^+$ ion bombardment. However, in all the studies just mentioned the authors investigated only the phase formation of $Pd_2Si$ and PdSi or the phase transition, and did not report on the mixing mechanisms involved, such as isotropic cascade mixing or radiation-enhanced diffusion (RED).

The present study is intended to elucidate in more detail the basic mechanisms involved in the IBM process on the Pd–Si system. The characteristics of the ion beam mixed layers were investigated by Rutherford backscattering spectroscopy (RBS). The experimental results are quantitatively compared with the theoretical models for isotropic cascade mixing and RED.

## 2. Experimental procedure

A polished n-type Si(1 1 1) single crystal (resistivity 20 Ω cm) was cleaned by consecutive ultrasonic cleaning in trichloroethylene, acetone, methanol, and 18 MΩ deionized water. After a 10 sec etch in 5% aqueous HF, the silicon substrate was placed in a specially designed chamber [9] which allowed the sample to be positioned in front of the palladium evaporator or the ion mixing beam. During the mixing and evaporation process the sample was continuously rotated about the sample normal and positioned with respect to the deposition or mixng beam to obtain

0022–2461/89 $03.00 + .12 © 1989 Chapman and Hall Ltd.

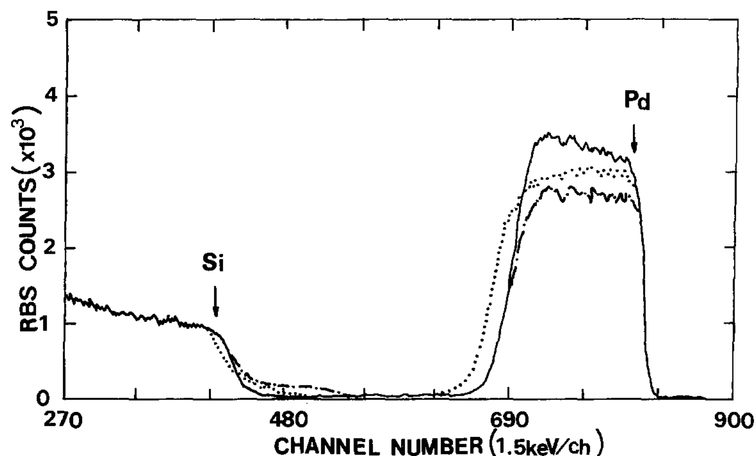


*Figure 1* Typical RBS spectra, normalized to a random silicon spectrum, for (——) an unirradiated sample and for samples mixing with (····) $3 \times 10^{15}$ and (—·—) $1 \times 10^{16}$ $Ar^+ cm^{-2}$ at 78 keV.

a laterally uniform mixed layer. The 45 nm thick palladium film was vapour-deposited on the silicon at a rate of 0.1 nm $sec^{-1}$ and then mixed. The deposition rate and the approximate thickness of the palladium film were measured by a vibrating quartz crystal deposition monitor.

Mixing was carried out at a pressure of $2 \times 10^{-7}$ torr at room temperature. To avoid sample heating due to ion bombardment, the silicon substrate was glued on a large copper heat sink (sample holder) with a thermally conductive compound. The film thickness of 45 nm was chosen so as to match with the projected range of the 78 keV $Ar^+$ ions, including the effects of straggling and sputtering. Doses from $1 \times 10^{15}$ to $1.5 \times 10^{16} cm^{-2}$ were used for mixing the bilayers of Pd–Si with an average beam current density of $1\,\mu A\,cm^{-2}$. The mixing beam was generated by a 150 keV ion implanter.

The mixing profiles were obtained using $He^+$ backscattering (RBS) with the target tilted to an angle of 78° to give an enhancement of the depth resolution by a factor of 4.8. A 1.4 MeV $He^+$ beam extracted from a 2 MeV Van de Graaff accelerator [10] was magnetically analysed and collimated to a 1 $mm^2$ spot on the sample. The energy of backscattered $He^+$ ions was analysed with a surface barrier detector mounted 10 cm from the target at a laboratory scattering angle of 160°. The energy resolution of the analysing system is about 16 keV.

## 3. Results and discussion

Ion beam mixing at the Pd–Si interface was characterized using RBS. Fig. 1 shows typical RBS spectra for an unirradiated sample and for samples irradiated with doses of $3 \times 10^{15}$ and $1 \times 10^{16} cm^{-2}$. All the spectra have been normalized to a random silicon spectrum obtained from an unmixed Pd–Si sample. The leading edge of the signals for the palladium and silicon elements are indicated by arrows in the figure. The portion of the RBS spectra for palladium and silicon are redrawn for clarity in Figs 2 and 3, respectively. The areas of spectra for unirradiated and irradiated samples should remain the same if sputtering during $Ar^+$ implantation does not occur. But the total palladium yield has decreased after irradiation (see Figs 1 and 2) due to sputtering during $Ar^+$ ion bombardment. It is found that the sputtered thickness of palladium, which is increased with dose, is determined to be 9 nm at $1.5 \times 10^{16} Ar^+ cm^{-2}$ from the area analysis. Therefore, silicon signals should move to higher energies due to less backscattered energy loss arising from the decreased thickness of palladium. In order to examine the shift of silicon signal associated with true mixing, the silicon signals in Fig. 1 should shift to lower energies by amounts corresponding to the sputtered thickness at a given dose if we want real spectra for silicon having no sputtering as shown in Fig. 3.

It can be seen from Figs 2 and 3 that $Ar^+$ ion irradiation has caused the broadening of the RBS spectra for palladium and silicon. It is also apparent that the signal height in the region of palladium after ion bombardment is reduced with increasing ion dose, presumably due to reduced concentration as the palladium is redistributed. Finally, the signal position of the rear edge for palladium is shifted to lower energy after the lower-dose ion bombardment, while the front edge of silicon is shifted to a higher energy. These observations clearly indicate that intermixing has occurred through the Pd–Si interface as a result of $Ar^+$ ion bombardment at room temperature.

In the case of the higher dose of $1 \times 10^{16} cm^{-2}$, the total palladium yield is reduced and the rear edge of the palladium signal has moved to higher energy due to the sputtering at the surface during $Ar^+$ bombardment. Also, the front edge of the silicon signal is consistent with silicon having moved through the palladium to the surface of the sample as shown in Figs 1 and 3. At this dose, the RBS spectra show clearly a well-defined plateau on the front edge of the silicon signal and over the entire range of the palladium signal, which can be interpreted as due to the formation of a uniform $Pd_mSi_n$ layer by IBM at room temperature (see also Fig. 1). The stoichiometry of the $Pd_mSi_n$ compound formed by IBM can be easily determined from the uniform spectrum heights and the atomic numbers for palladium and silicon [11]:

$$\frac{m}{n} = \frac{H_{Pd}}{H_{Si}} \left(\frac{Z_{Si}}{Z_{Pd}}\right)^2 \frac{[\varepsilon_0]_{Pd}^{Pd_2Si}}{[\varepsilon_0]_{Si}^{Pd_2Si}} \qquad (1)$$

where $H_{Pd}$ and $H_{Si}$ are the signal heights of palladium and silicon, respectively, $Z_{Pd}$ and $Z_{Si}$ are their atomic numbers, and $[\varepsilon_0]_{Pd}^{Pd_2Si}$ and $[\varepsilon_0]_{Si}^{Pd_2Si}$ are the surface energy approximations to the stopping cross-section factors for particles scattered from palladium and silicon atoms, in the $Pd_2Si$ layer, respectively. From the

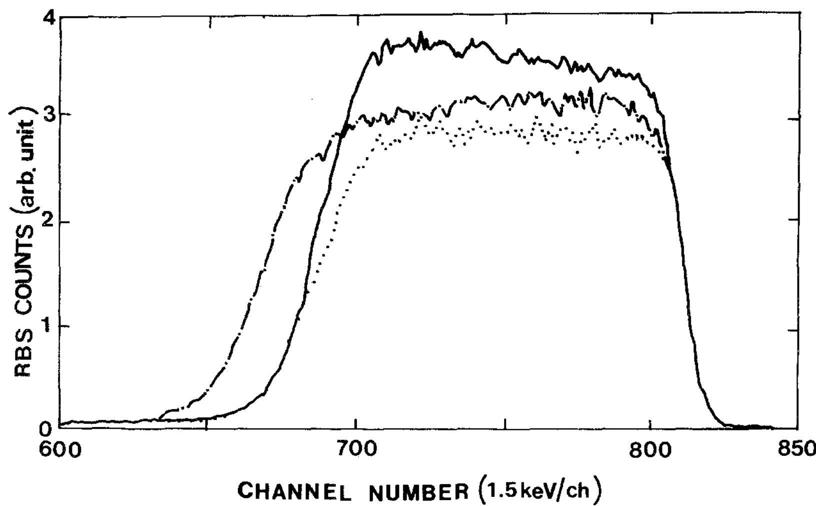


*Figure 2* The palladium region of the RBS spectra for (——) an unirradiated sample and for mixed samples with doses of (—·—) $3 \times 10^{15}$ and (···) $1 \times 10^{16}$ $Ar^+ cm^{-2}$ at 78 keV.

calculation using Equations 1, the ratio $m/n$ is found to be 2.1 which can be considered to be 2 within the experimental error. This result is consistent with the formation of $Pd_2Si$ as the initial compound resulting from $Ar^+$ ion beam mixing, and also TEM diffraction identifies the phase as $Pd_2Si$ [12]. In view of the fact that $Pd_2Si$ is normally formed at elevated temperatures (above 200° C) for the conventional furnace annealing method, the formation of this equilibrium compound at room temperature by IBM is very interesting from the viewpoint of technology. Furthermore, the stoichiometry of this initial compound formed in the mixed layer is identical with that of the first phase formed by thermal annealing, which implies that the Walser–Bene rule [13] describing the first thermal phase as deduced from the phase diagram is still obeyed in the IBM process, even though this process is a kind of non-equilibrium method.

We have previously discussed the phase formation, solid-solution formation and interfacial reaction of the Pd–Si bilayer system in more detail in a separate paper [14]. A brief summary of our results is as follows. The palladium penetrates approximately 3 nm deep into the silicon from the Pd–Si interface, while the silicon moves 14 nm across the interface already in the as-deposited state, corresponding to the formation of a $Pd_2Si$ layer 4.4 nm thick during deposition. After $Ar^+$ ion bombardment at a dose of $1 \times 10^{16} cm^{-2}$, the thickness of the $Pd_2Si$ layer is found to be 48 nm. The reacted thicknesses of palladium and silicon needed to form this $Pd_2Si$ layer should be 32.7 and 22.2 nm, respectively. These results imply that the dominant moving species is silicon atoms in the interfacial mixing of Pd–Si.

In this paper we intend to elucidate the ion beam mixing mechanisms operating, such as isotropic cascade mixing, radiation-enhanced diffusion, vacancy production and its related diffusivity. The area of the RBS spectra for the as-deposited state and the ion-bombarded samples should remain the same if sputtering during $Ar^+$ bombardment does not occur. Then the degree of mixing can be represented by the changes in spectral area for the respective samples. However, this method does not work at higher doses because of sputtering as can be seen in Fig. 1 for a dose of $1 \times 10^{16} cm^{-2}$ where the palladium signal is reduced in width. Instead, the amount of intermixing due to the $Ar^+$ bombardment will be characterized by the increase in the variance, $\Omega^2$, of the edge signal in the RBS spectra for palladium and silicon:

$$\Omega^2 = \Omega^2(\phi) - \Omega^2(0) \quad (2)$$

where $\Omega^2(\phi)$ and $\Omega^2(0)$ are deduced by measuring the half-width between the 16% and 84% points of the low-energy edge of the palladium signal, and the high-energy edge of the silicon signal, for the irradiated (dose $\phi$) and unirradiated (dose 0) sample. Then, the variance $\Omega^2$ in $(\text{energy})^2$ is converted to variance $\sigma^2$ in $(\text{length})^2$ by the following relation

$$\sigma^2 = \frac{\Omega^2}{(N[\varepsilon])^2} \quad (3)$$

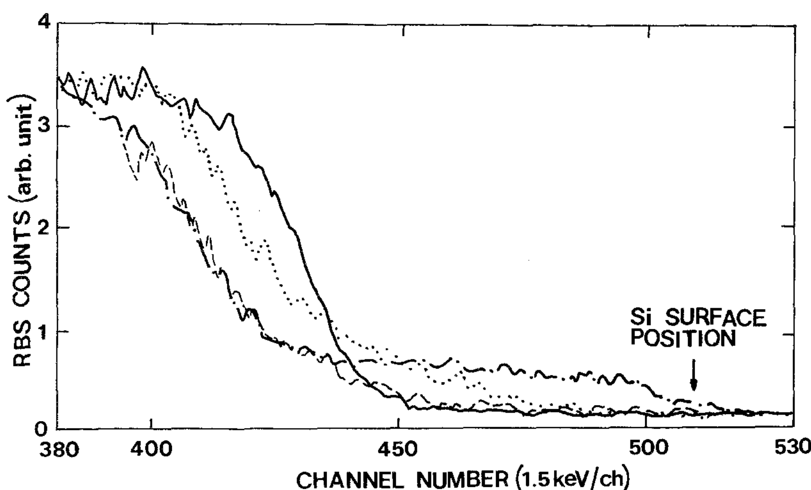


*Figure 3* The high-energy edge of the silicon region of the RBS spectra for (——) an unirradiated sample and for mixed samples with doses of (···) $3 \times 10^{15}$, (—·—) $1 \times 10^{16}$ and (– – –) $1.5 \times 10^{16}$ $Ar^+ cm^{-2}$ at 78 keV. The silicon surface position for a $He^+$ ion of 1.4 MeV is shown by the arrow.

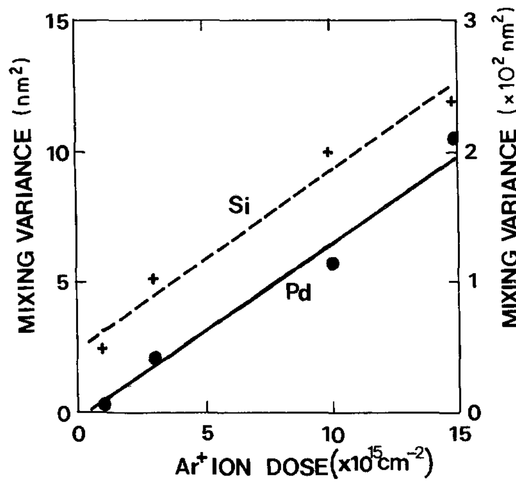


*Figure 4* The experimental mixing variance for (●) palladium (left-hand scale) and (+) silicon (right-hand scale) plotted as a function of dose for 78 keV $Ar^+$ irradiation at room temperature.

where $N$ and $[\varepsilon]$ are, respectively, the atomic number density and the stopping cross-section factor of the palladium and silicon for $He^+$ backscattering. The experimental results for the palladium and silicon variance at various values of dose $\phi$ are shown in Fig. 4. These results clearly show that the intermixing amount increases linearly with increasing dose. Also, the mixing amount for silicon is larger than that of palladium by a factor of 30, which implies that the dominant moving species should be silicon. We present in the following discussion a qualitative and quantitative analysis of the dose dependency and this difference of mixing amount between palladium and silicon.

Ion bombardment may greatly accelerate the diffusion of substitutional or interstitial atoms at relatively low temperatures. The increased vacancy concentration produced during the ion bombardment causes a proportional increase in diffusion by the vacancy mechanism or the interstitial mechanism. This process comprises what is usually referred to as radiation-enhanced diffusion. The atomic diffusivity under the conditions of RED is governed by the production rate of mobile vacancies and interstitials, by the migration enthalpy of these defects, and by the probabilities of their annihilation by recombination with each other or into immobile sinks such as the surface or dislocations.

Myers [15] has obtained an analytical expression for the enhanced diffusion constant $D$. At sufficiently high temperatures, normal thermal diffusion dominates, that is, the unenhanced diffusivity applies as given by

$$D = D_0 \exp\left(\frac{-Q}{kT}\right) \tag{4}$$

where $D_0$ is the pre-exponential constant, and the activation energy for diffusion, $Q$, is the sum of vacancy formation enthalpy $E_v^f$ and vacancy migration enthalpy $E_v^m$. At a somewhat lower temperature when the diffusion is enhanced by radiation, and point defects are annihilated mostly at fixed sinks, the diffusion constant can be written as

$$D = 2\alpha P l^2 \tag{5}$$

Here $\alpha$ is the fraction of the point defects which escape the cascade to migrate freely through the lattice, $l$ is a characteristic diffusion length to fixed sinks ($1/l^2$ is the density of sink sites), and $P$ is the production rate of vacancy–interstitial pairs, which can be calculated from the modified Kinchin–Pease relation [16]

$$P = \frac{0.4}{NE_d} S_n \dot{\phi} \tag{6}$$

In Equation 6, $N$ is the atomic density of the material, $E_d$ is the effective threshold displacement energy, $\dot{\phi}$ is the ion flux and $S_n$ is the nuclear stopping power of the material for the incident ion. Finally, at an even lower temperature where annihilation of vacancies occurs principally by recombination, the diffusivity is expressed by

$$D = \left(\frac{\alpha P D_v}{\pi N R_{iv}}\right)^{1/2} \tag{7}$$

yielding an activation enthalpy of one-half the vacancy migration enthalpy. In Equation 7 $R_{iv}$ is the vacancy–interstitial separation at which spontaneous recombination occurs. The value of $R_{iv}$ is approximately 1 nm, corresponding to a recombination volume of 100 atoms as is typically reported [16], and $D_v$ is the vacancy diffusivity described by [17]

$$D_v = a^2 f_v \exp\left(-\frac{E_v^m}{kT}\right) \tag{8}$$

where $a$ is the lattice constant and $f_v$ is the jump frequency factor for a vacancy. Under the conditions of RED dominated by interstitial diffusion, $D_v$ has to be replaced by $D_i$ (interstitial diffusivity) described by [17]

$$D_i = 0.1 a^2 f_i \exp\left(-\frac{E_i^m}{kT}\right) \tag{9}$$

where $f_i$ is the jump frequency factor for interstitials and $E_i^m$ is the migration enthalpy for interstitials.

At still lower temperatures below the recombination region, isotropic cascades contribute to short-range mixing, which can be calculated by the well-known formula [18] for the binary collision approximation:

$$D = \frac{\Gamma_0}{6} \frac{S_n}{N} \zeta_{21} \frac{R_{iv}^2}{E_d} \dot{\phi} \tag{10}$$

where $\Gamma_0 = 0.608$ and $\zeta_{21} = [4m_1m_2/(m_1 + m_2)^2]^{1/2}$. Here $m_1$ and $m_2$ are the atomic mass numbers for incident ion and target atom, respectively. Reasonable values for the various parameters in these equations are listed in Table I. In Table I the values for $S_n$ were calculated using the TRIM code, and the value of $l$ for silicon is assumed to be $(1/6^{1/2}) \times 10^{-6}$ cm, because the total vacancy density on the palladium side is larger than that for the silicon side by a factor of 6 as described in our previous paper [14].

First, using Equations 4, 5, 7 and 10 for vacancy diffusion and with the appropriate values form Table I, the diffusivity for palladium as a function of reciprocal temperature was calculated as shown in Fig. 5. The experimental value is shown for comparison, and was calculated from Fig. 4 using the relation between $\Omega^2$ and $D$ as in the case of the error function [19];

$$\Omega^2 = 2Dt \tag{11}$$

TABLE I Basic parameters used in calculations

| Parameter | Notation | Values | | References |
|---|---|---|---|---|
| | | Pd | Si | |
| Pre-exponential factor ($cm^2 sec^{-1}$) | $D_0$ | 0.21 | 1460 | [20] |
| Thermal activation enthalpy (eV) | $Q$ | 2.76 | 5.02 | [20] |
| Migration enthalpy for vacancy (eV) | $E_v^m$ | 1.47 | 1.08 | [17, 21] |
| Migration enthalpy for interstitial (eV) | $E_i^m$ | ? | 0.6 | [17] |
| Nuclear stopping power ($eV nm^{-1}$) | $S_n$ | 1033 | 510 | |
| Lattice constant (nm) | $a$ | 0.389 | 0.543 | |
| Jump frequency factor for vacancy ($sec^{-1}$) | $f_v$ | $5 \times 10^{13}$ | $5 \times 10^{13}$ | [22] |
| Jump frequency factor for interstitial ($sec^{-1}$) | $f_i$ | $5 \times 10^{12}$ | $5 \times 10^{12}$ | [22] |
| Effective displacement energy (eV) | $E_d$ | 47 | 21.7 | [23] |
| Characteristic diffusion length (cm) | $l$ | $10^{-6}$ | $\frac{1 \times 10^{-6}}{6^{1/2}}$ | [24] |
| Fraction of active point defects | $\alpha$ | 0.1 | 0.1 | [15, 25] |

where $t$ is $\phi/\dot{\phi}$. The various temperature regimes discussed above are indicated on the figure. Fig. 5 shows that only the isotropic cascade mixing occurs below 600 K. Thus one can easily conclude that the palladium atoms diffuse across the Pd–Si interface by the cascade mixing mechanism at room temperature. Furthermore, the experimental value is in good agreement with the calculated value in the isotropic cascading mixing regime. Next we compared the experimental dose dependency of palladium as shown in Fig. 4 with calculated values using Equation 11 and the calculated value of $D$ ($1.78 \times 10^{-17} cm^2 sec^{-1}$) obtained in the cascade mixing region. The results are plotted in Fig. 6. The combined results of Figs 5 and 6 strongly indicate that the interdiffusion of palladium atoms occurs via the isotropic cascade mixing mechanism.

Second, using Equations 4, 5, 7 and 10 for vacancy diffusion, and taking the appropriate values from Table I, the diffusivity for silicon as a function of reciprocal temperature was calculated as shown in Fig. 7. Again, the experimental value using Equation 11 is shown for comparison. This figure shows that isotropic cascade mixing occurs below 420 K, RED associated with vacancy diffusion occurs between 770 and 420 K, and RED in the regime of annihilation to the fixed sinks occurs between 1430 and 770 K. As can be seen in Fig. 7, the experimental result does not coincide with any calculated values in these regions. In the cascade mixing region, the experimental result is higher by a factor of 20. This implies that the interdiffusion of silicon cannot be explained by RED via the vacancy diffusion mechanism, or by isotropic cascade mixing as was seen for palladium.

In an effort to understand the origin of this discrepancy, the enhanced diffusion associated with the interstitial mechanism is considered. Thus we have calculated the diffusivity for silicon based on the interstitial diffusion using Equations 4, 5, 7 and 10, choosing the appropriate values from Table I for interstitials. In the calculation of Equation 7, Equation 9 is used instead of Equation 8 because of interstitial diffusion. The results are shown in Fig. 7. In this case, the temperature range for the interstitial RED region is found to be from 500 K down to 200 K. At room temperature the diffusivity is larger than that of the cascade region by a factor of 15, and is very close to the experimental point. Thus we conclude that silicon atoms interdiffuse into the palladium matrix by RED via an interstitial mechanism.

We compare the experimental dose dependence of $\Omega^2$ for silicon with the theoretical values obtained

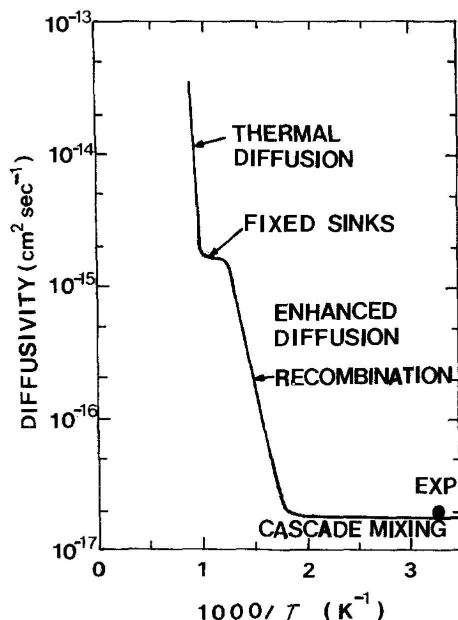


*Figure 5* The calculated diffusivity as a function of $10^3/T$ for 78 keV $Ar^+$ irradiated palladium ($1 \mu A cm^{-2}$). The various regimes are indicated in detail. The experimental result is shown by a solid circle.

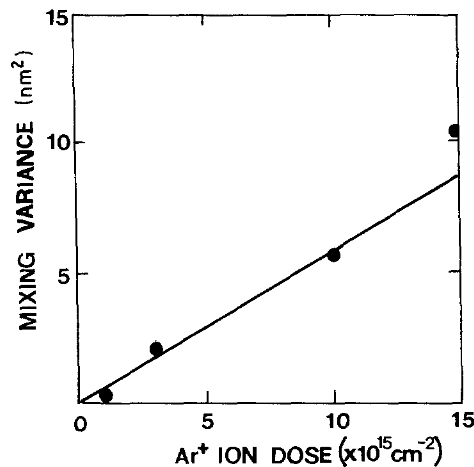


*Figure 6* A comparison of (●) the experimental dose dependence of the mixing variance with (——) the theoretical model for palladium.

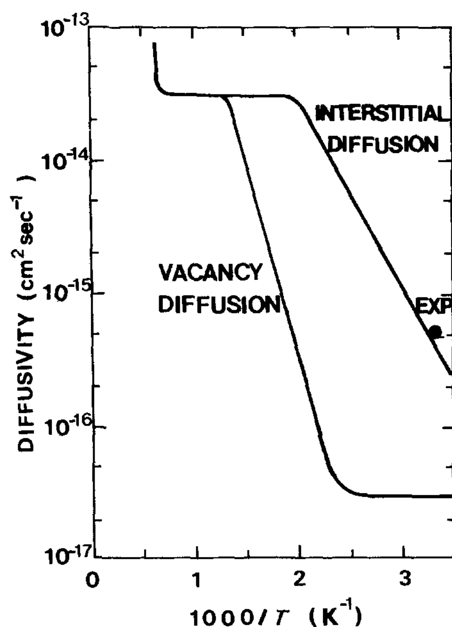


*Figure 7* The calculated interstitial and vacancy diffusivity as a function of $10^3/T$ for 78 keV $Ar^+$ irradiated silicon (1 $\mu A\,cm^{-2}$). The experimental result is shown by a solid circle.

from Equation 11, using the calculated value of $D$ from Fig. 7 ($4 \times 10^{-16} cm^2 sec^{-1}$) for the interstitial RED region. The results, plotted in Fig. 8, show reasonable agreement between theory and experiment, although the absolute values of the experimental points are somewhat higher than the calculated ones. We suppose that this discrepancy might be due to the contribution of a chemical driving force (heat of mixing enthalpy [26]). This contribution, as well as the temperature dependence of $\Omega^2$, still need further study and are the subject of continuing work at our laboratory.

## 4. Conclusions

We observe that $Ar^+$ ion bombardment onto a Pd–Si bilayer leads to the formation of a $Pd_2Si$ layer at the Pd–Si interface. The experimental mixing variance, $\Omega^2$, for silicon is larger than that of palladium by a factor of 30, because different diffusion mechanisms are involved for silicon and palladium. From a comparison between experimental results and model calculations, the diffusion of palladium is thought to be associated with an isotropic cascade mixing mechanism, a model of which successfully explains the dose dependence of $\Omega^2$ for palladium. However, the diffusion of silicon appears to be related to radiation-enhanced diffusion via an interstitial mechanism. These two models explain successfully the mixing behaviour and the dose dependence for palladium and silicon in the Pd–Si bilayer.

## Acknowledgements

This study was supported in part under a contract with the Idaho National Engineering Laboratory EG & G Idaho, Inc. supported through the US Department of Energy under Contract No. DE-Ac07-761D01570. We also wish to express deep gratitude to the Korea Science and Engineering Foundation for financial support.

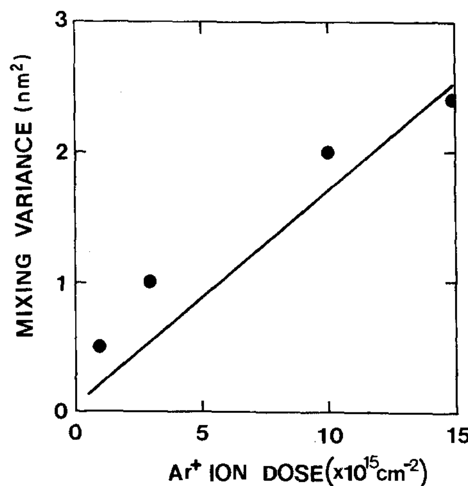


*Figure 8* A comparison of (●) the experimental dose dependence of the mixing variance with (——) the theoretical model for silicon.

## References

1. K. MAEX, L. van den HOVE and R. E. de KEERSMAECKER, *Thin Solid Films* **140** (1986) 149.
2. H. ISHIWARA, K. HIKOSAKA, M. NAGATOMO and S. FURUKAWA, *Surf. Sci.* **86** (1979) 711.
3. H. ISHIWARA, *Thin Solid Films* **92** (1982) 147.
4. K. HIKOSAKA, H. ISHIWARA and S. FURUKAWA, *Radiat. Eff.* **51** (1980) 253.
5. G. A. HUTCHINS and A. SHEPOLA, *Thin Solid Films* **18** (1973) 343.
6. D. H. LEE, R. R. HART, D. A. KIEWIT and O. J. MARSH, *Phys. Status Solidi (a)* **15** (1973) 645.
7. W. F. van der WEG, D. SIGURD and J. W. MAYER, in "Application of Ion Beams to Metals", edited by S. T. Picraux (Plenum, New York, 1974) p. 209.
8. B. Y. TSAUR, S. S. LAU and J. W. MAYER, *Appl. Phys. Lett.* **35** (1979) 225.
9. C. N. WHANG, R. Y. LEE, H. K. KIM and R. J. SMITH, *J. Korean Phys. Soc.* **20** (1987) 339.
10. R. J. SMITH, C. HENNESSY, M. W. KIM, C. N. WHANG, M. WORTHINGTON and XU MINGDE, *Rev. Sci. Instr.* **58** (1987) 2284.
11. W. K. CHU, J. W. MAYER and M. A. NICOLET, "Backscattering Spectrometry" (Academic, New York, 1978) pp. 79 and 115.
12. R. Y. LEE, C. N. WHANG, H. K. KIM and R. J. SMITH, *Nucl. Instrum. Meth.* **B38** (1988) 661.
13. R. M. WALSER and R. W. BENE, *Appl. Phys. Lett.* **28** (1976) 624.
14. R. Y. LEE, C. N. WHANG, H. K. KIM and R. J. SMITH, *J. Mater Sci.* in press.
15. S. M. MYERS, *Nucl. Instrum. Meth.* **168** (1980) 265.
16. P. SIGMUND, *Appl. Phys. Lett.* **14** (1969) 114.
17. N. Q. LAM and G. K. LEAF, *J. Mater. Res.* **1** (1986) 251.
18. P. SIGMUND and A. GRAS-MARTI, *Nucl. Instrum. Meth.* **182/183** (1981) 25.
19. M. A. NICOLET, "Ion Mixing and Surface Layer Alloying" (Noyes, Park Ridge, 1984) p. 12.
20. N. L. PETERSON, *J. Nucl. Mater.* **69/70** (1978) 3.
21. P. H. DEDERICHS, *ibid.* **69/70** (1978) 176.
22. N. Q. LAM, K. JANGHORBAN and A. J. ARDELL, *ibid.* **101** (1981) 314.
23. H. H. ANDERSEN, *Appl. Phys.* **18** (1979) 131.
24. H. WIEDERSHICH, *Nucl. Instrum. Meth.* **B7/8** (1985) 1.
25. F. BESENBACHER, J. BØTTIGER, S. K. NIELSEN and H. J. WHITLOW, *Appl. Phys.* **A29** (1982) 141.
26. A. R. MIEDEMA, *Philips Tech. Rev.* **8** (1976) 36.

*Received 14 December 1987*
*and accepted 6 May 1988*